

FEATURE ARTICLE

Electronic Wave Functions in Semiconductor Clusters: Experiment and Theory

Louis Brus

AT&T Bell Laboratories, Murray Hill, New Jersey 07974 (Received: December 26, 1985)

In this manuscript we critically review, and discuss in greater detail, recent experimental and theoretical work in the size-dependent development of bulk electronic properties in semiconductor crystallites of ~ 15 Å to several hundred angstroms. A special effort is made to explain semiconducting electronic properties using chemical valence terminology. These crystallites can be termed "clusters" because they are too small to have bulklike electronic wave functions even though they exhibit bulklike crystal structure. The principal experimental evidence comes from the recent discovery that liquid-phase precipitation reactions can be controlled to make and stabilize crystalline semiconductor clusters in this size range. The cluster electronic properties can be studied optically in dilute colloidal solutions. The cluster internal crystal structure is directly revealed by transmission electron microscopy. The results indicate that the approach of cluster electronic wave functions to the bulk Bloch molecular orbitals is exceedingly slow as a function of cluster size. This result can be analytically predicted in terms of the intrinsic electron delocalization present in crystalline materials with strong, directional chemical bonding.

Introduction

Benzene is especially stable due to π electron resonance delocalization on the ring. A single sheet of graphite can be viewed as a strongly bonded system of rings in which greater spatial π electron delocalization is possible. While benzene has discrete π and π^* molecular orbitals (MOs), in the graphite sheet these bonding and antibonding orbitals are so numerous as to merge into effective continua labeled the valence and conduction bands, in solid-state language.¹ In an N ring fragment of a graphite sheet, the highest occupied MO (HOMO) moves up in energy and the lowest antibonding MO (LUMO) moves down in energy, as N increases. As a consequence the HOMO \rightarrow LUMO excited state comes down in energy as a function of N . For example, this state lies near 260 nm in benzene, near 580 nm in pentacene, and further to the red in larger fragments. In the limit that $N \rightarrow \infty$, the HOMO \rightarrow LUMO transition energy actually goes to zero. A single graphite sheet is called a "semimetal" because the valence band top just touches the conduction band bottom.¹ If the HOMO \rightarrow LUMO transition energy remains nonzero in the limit of $N \rightarrow \infty$, as in the case of hexagonal boron nitride, the infinite sheet falls into the semiconductor/insulator category.

The unique physical properties of diamond crystals are also a direct consequence of electron delocalization. The C atom hybridization is sp^2 in graphite, and sp^3 in diamond. Diamond has a tetrahedral crystal structure giving maximum overlap of the sp^3 orbitals. The result is extensive valence electron delocalization in three dimensions. One measure of the strength of this interaction is the 7.4-eV/atom atomization energy of a diamond crystal. Another measure is diamond's extreme hardness, resulting from a deep and steep potential energy curve in the ground electronic state. In Figure 1 a correlation diagram relating the diamond crystal MOs to the orbitals of separated C atoms is shown. This diagram is modified slightly from the 1935 diagram of the quantum chemist G. Kimball.² At the actual crystal C-C bond length, the valence band of bonding MOs is fully 35 eV wide. There is an energy gap of 5.4 eV between the full valence band and the empty conduction band. This large gap makes diamond an insulator.

Silicon sits below carbon in the periodic table. Silicon has the same crystal structure and valence electron delocalization as

diamond, although the sp^3 overlaps are not as large and the bonds are weaker. Crystalline Si, a semiconductor with a band gap of about 1 eV, is extremely well characterized because of its importance in the computer/telecommunications industry. Nevertheless, the electronic properties of small silicon (or diamond) crystallites (~ 100 Å) have never been reported.³ The preceding discussion of spatial delocalization in graphite illustrates how MOs of small silicon and diamond crystallites should be quite sensitive to the physical size of that crystallite. This size sensitivity, a direct consequence of quantum mechanics, is one aspect of the "cluster" problem—the transformation from molecular to bulk solid-state properties as a function of size.

Small Si_n clusters serve to illustrate a second aspect of the cluster problem. Recent accurate calculations on the equilibrium structures of the $n \leq 10$ clusters predict that these clusters are not fragments of the bulk tetrahedral lattice structure.⁴ The predicted structures are compact shapes of high symmetry tending to maximize the number of (strained) Si-Si bonds and nearest neighbors. Presumably tetrahedral fragment cluster structures will only become favorable for $n \gg 10$, where spatial delocalization along longer networks is possible. This result suggests that, for the relatively open diamond and zinc-blende lattices (Si, Ge, GaAs, CdS, InSb, etc.), there will be two cluster size regimes: (a) $n \leq 30$ – 10^3 (?) where the bulk lattice structure is not found and the properties are entirely molecular, and (b) 30 – 10^3 (?) $\leq n < 10^5$ where the bulk lattice structure exists but the bulk electronic properties are not yet achieved. The recent conjecture by Smalley and co-workers⁵ on an icosahedral structure for a C_{60} cluster suggests that unique cluster "molecules" can be made at intermediate sizes. As we shall see, in the second regime recent experiments indicate that II-VI crystallites with more than ~ 200 atoms have the bulk lattice structure (when made by liquid-phase precipitation); however, the electronic properties have hybrid molecular/solid-state character. We focus on this second regime in this article.

These ideas have been understood in principle for decades. However, there has been a recent burst of excitement focused on experimental observation of the transformation from molecular

(1) Spain, I. L. In *Chemistry and Physics of Carbon*, Vol. 16, Walker, P., Thrower, P., Eds.; Marcel Dekker: New York, 1981, Chapter 2.
(2) Kimball, G.E. *J. Chem. Phys.* 1935, 3, 560.

(3) The first reports of Si cluster mass spectra have appeared: Bloomfield, L. A.; Freeman, R. R.; Brown, W. L. *Phys. Rev. Lett.* 1985, 54, 2246. Martin, T. P.; Schaber, H. *J. Chem. Phys.* 1985, 83, 855.
(4) Ragavachari, K.; Logovinsky, V. *Phys. Rev. Lett.* 1985, 117, 29.
(5) Kroto, H. W.; Heath, J. R.; O'Brien, S. C.; Curl, R. F.; Smalley, R. E. *Nature (London)* 1985, 318, 162.

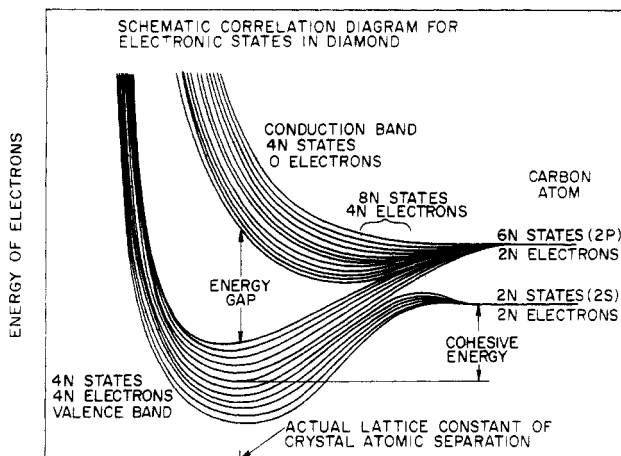


Figure 1. Schematic correlation diagram relating the valence and conduction bands of diamond to the sp^3 orbitals of C atom. Adapted from ref 2.

to solid-state electronic properties in strongly bonded materials—metals and semiconductors. There are two experimental approaches to this problem. One involves atomic aggregation in beams and supersonic jets, and attempts to build up the solid state one atom at a time.^{3,5-9} Novel results have been reported involving surface reactivity and structural magic numbers in the past 2 years. This technique is clearly quite powerful.

The second method comes, somewhat improbably, from the area of colloid chemistry, where for about a decade there has been an active effort in the surface photochemistry of semiconductor suspensions.¹⁰⁻¹² These particles, typically of ~ 100 Å and larger, appear to behave as bulk semiconductors. However, in 1983 it was discovered that certain homogeneous precipitation reactions could be controlled to give tiny ~ 15 – 50 Å-diameter crystallites of the bulk lattice structure.¹³ Remarkably these crystallites did not have the electronic spectra of the bulk material even though they exhibited the same unit cell and bond length as the bulk semiconductors. It was concluded that these crystallites are *clusters* in which complete electron delocalization has not yet occurred.¹³ The crystallite “band gap” was observed to be several tenths of an electronvolt above the bulk gap even in crystallites containing a thousand atoms. In this article we discuss the growing effort in colloidal cluster synthesis and characterization, and the theory of cluster quantum size effects.

Experimental Observations

Synthesis. The sulfides and selenides of Zn, Cd, Pb, etc. have been explored in greater detail because of the relative simplicity (in hindsight) of the colloidal preparations, and the advanced state of the bulk solid-state physics literature for these crystals.¹³⁻²⁰ The

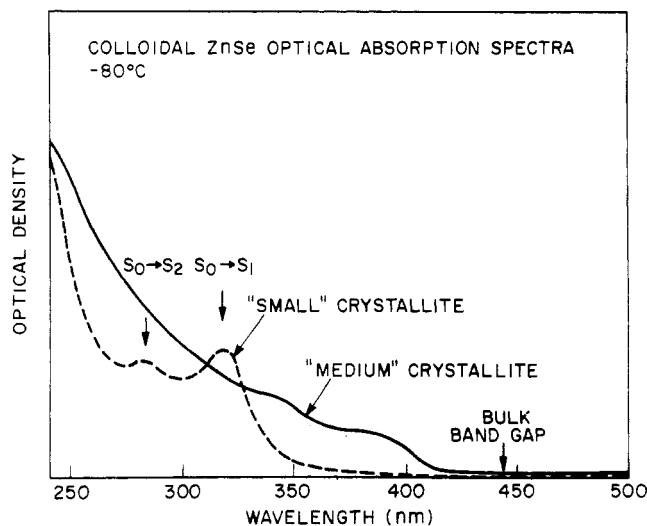


Figure 2. Size-dependent electronic absorption spectra of colloidal ZnSe clusters. Adapted from ref 34.

comparison between crystallite and bulk optical properties is unambiguous. There have also been initial reports of cluster quantum size effects in the optical spectra of the silver halides,²⁰ the phosphides and arsenides of Zn and Cd,^{21,22} CuCl,^{23,24} the layered semiconductor PbI₂,²⁵ and Fe₃O₂.²⁶ Careful structural and size measurements have been carried out in only a few of these experiments. Nevertheless, “arrested precipitation” has become a technique of wide utility. Solid-state precipitation reactions also yield clear optical evidence for clusters.^{23,24,27}

Our basic experimental strategy is to undertake synthetic and spectral characterization in the same liquid medium, avoiding physical manipulation and aggregation of the tiny crystallites. Thermal coagulation and Ostwald ripening can be controlled via double-layer repulsion of individual crystallites, by carrying out synthesis at low temperature in nonaqueous solvents, and by adsorption of foreign stabilizing molecules. In the case of PbI₂ and CdS, there is clear evidence for “magic numbers” in the initially precipitated clusters.^{18,25} Henglein and co-workers have shown the value of complexation with hexametaphosphate anion in stabilizing aqueous colloids of clusters, and in stabilizing “powders” of clusters made by solvent evaporation.

It is fortuitous that solvents such as 2-propanol, and ethanol-methanol mixtures, that are useful for stabilization of the smallest crystallites, also have the property of forming clear organic glasses when cooled. Thus it is possible to synthesize crystallites in a cold, viscous liquid just above its freezing point, and then cool further to cryogenic temperatures for absorption, Raman, and luminescence measurements. The detailed chemical kinetic mechanism of homogeneous precipitation is not known. The first reports of nucleation observation in real time are just appearing.^{28,29}

Optical Spectroscopy. The basic experimental relationship between size and optical spectra was first worked out and confirmed for ZnS and CdS.^{13-19,27} The characteristic result is shown in Figure 2 for ZnSe.¹⁶ The band gap of the bulk crystal is 2.8 eV, corresponding to an optical absorption threshold at about 430 nm. The bulk crystal absorption has a small step at this threshold, and then shows a smooth, continuous absorption rising to higher energy. The 100-Å diameter and larger crystals show bulklike spectra. It is probable that, with high resolution, deviations from

(6) Knight, W. D.; Clemenger, K.; deHeer, W. A.; Saunders, W. A.; Chou, M. Y.; Cohen, M. L. *Phys. Rev. Lett.* **1984**, *52*, 2141.

(7) Whetten, R. L.; Cox, D. M.; Trevor, D. J.; Kaldor, A. *Phys. Rev. Lett.* **1985**, *54*, 1494.

(8) Martin, T. P. *Ber. Bunsenges. Phys. Chem.* **1984**, *88*, 300.

(9) Liu, K.; Parks, E. K.; Richtsmeier, S. C.; Pobo, L. G.; Riley, S. J. *J. Chem. Phys.* **1985**, *83*, 2882.

(10) Henglein, A. *Pure Appl. Chem.* **1984**, *56*, 1215.

(11) Moser, J.; Gratzel, M. *J. Am. Chem. Soc.* **1983**, *105*, 6547.

(12) Fox, M. A.; Lindig, B.; Chen, C. C. *J. Am. Chem. Soc.* **1982**, *104*, 5828.

(13) Rossetti, R.; Nakahara, S.; Brus, L. E. *J. Chem. Phys.* **1983**, *79*, 1086.

(14) Rossetti, R.; Ellison, J. L.; Gibson, J. M.; Brus, L. E. *J. Chem. Phys.* **1984**, *80*, 4464.

(15) Rossetti, R.; Hull, R.; Gibson, J. M.; Brus, L. E. *J. Chem. Phys.* **1985**, *82*, 552.

(16) Chestnoy, N.; Hull, R.; Brus, L. E. *J. Chem. Phys.*, in press.

(17) Weller, H.; Koch, U.; Gutierrez, M.; Henglein, A. *Ber. Bunsenges. Phys. Chem.* **1984**, *88*, 649.

(18) Fojtik, A.; Weller, H.; Koch, U.; Henglein, A. *Ber. Bunsenges. Phys. Chem.* **1984**, *88*, 969.

(19) Nozik, A. J.; Williams, F.; Nenadovic, M. T.; Rajh, T.; Micic, O. I. *J. Phys. Chem.* **1985**, *89*, 397.

(20) Rossetti, R.; Hull, R.; Gibson, J. M.; Brus, L. E. *J. Chem. Phys.* **1985**, *83*, 1406.

(21) Weller, H.; Fojtik, A.; Henglein, A. *Chem. Phys. Lett.* **1985**, *117*, 485.

(22) Fojtik, H.; Weller, H.; Henglein, A. *Chem. Phys. Lett.* **1985**, *120*, 552.

(23) Itoh, T.; Kirihaara, T. *J. Lumin.* **1984**, *31/32*, 120.

(24) Ekimov, A. I.; Onushchenko, A. A. *JETP Lett.* **1981**, *34*, 346.

(25) Sandroff, C. J.

(26) Bahnmann, D., private communication.

(27) Ekimov, A. I.; Onushchenko, A. A. *JETP Lett.* **1984**, *40*, 1136.

(28) Tanaka, T.; Masashi, M. *J. Photog. Sci.* **1983**, *31*, 13.

(29) Tanaka, T.; Iwasaki, M. *J. Imaging Sci.* **1985**, *29*, 86.

bulk behavior just above the band gap would be seen even above 100 Å. However, in "medium"-sized crystals, typically of 40–50 Å, the apparent absorption edge begins to shift blue as shown in the figure at low resolution. For "small" crystallites, typically of 20–30-Å diameter, the blue shift is more than 1 electronvolt. Peaks appear in the spectra, representing discrete excited electronic states. In the figure the first and second excited electronic states of the cluster are partially resolved. The apparent continuous absorption at higher energy rises faster than does the corresponding bulk absorption. As previously noted, these changes have now been observed systematically in a wide variety of semiconductors. In small band gap materials the broadening processes appear to be so severe that the absorption shifts to higher energy without simultaneous appearance of discrete peaks.

Are these changes electromagnetic in nature, or are they related to cluster electronic structure? At this point, we briefly introduce a third aspect of the cluster problem—the size-dependent interaction of the cluster with the electromagnetic field. The interaction Hamiltonian between a system of electrons (molecule or crystal) and the radiation field is

$$\hat{H}_{\text{int}} = \bar{\mathbf{A}} \cdot \bar{\mathbf{P}}$$

where $\bar{\mathbf{A}}$ is the field vector potential and $\bar{\mathbf{P}}$ is the electron momentum. In molecular spectroscopy, a nice simplification occurs in that \hat{H}_{int} is small enough to accurately be handled by perturbation theory. This perturbation expansion yields the well-known result that electric dipole transitions are strongest because they occur in first order. Magnetic dipole and electric quadrupole transitions are $\sim 10^{-4}$ as strong because they occur in second order, and higher moments are corresponding weaker.

In bulk solid-state physics this result is not valid; \hat{H}_{int} is large and must be incorporated into the zero-order wave functions. The basic nature of the electromagnetic field is changed by the presence of dense matter; this leads to phenomena, such as bulk and surface polaritons (plasmons), having no molecular analogy.

In cluster spectroscopy we must have a continuous transition between these two spectroscopic regimes as a function of cluster size. The first manifestation of this transition should be an increase in the strength of the higher order transition moments relative to electric dipole moments. When higher order moments become of equal magnitude, the cluster optical spectra change for purely electromagnetic reasons.

This shape-dependent transition is handled classically by Mie scattering theory. The material properties are embodied in the complex, wavelength-dependent dielectric coefficient. A general result is that the electric dipole term dominates in the limit that $R/\lambda \rightarrow 0$, where R is the crystallite radius. A quantitative calculation shows that little crystallites of our materials should have size-independent spectra in this region below 100 Å.¹⁴ The crystallites are molecules as far as the electromagnetic field is concerned. Thus we conclude that the experimental spectra must actually be changing for some chemical or electronic reason related to the structure of the crystallite.

Transmission Electron Microscopy. It is of paramount importance to know the structure of the crystallites produced by these "arrested precipitation" techniques. These clusters contain several hundred (or more) atoms, suggesting the use of X-ray or electron diffraction structural methods. Transmission electron microscopy (TEM) has become an essential tool in the characterization of interfaces and surfaces at the atomic level.³⁰ The point-to-point resolution is currently ≈ 1.5 Å, and single atoms of high Z elements can be directly imaged. The usefulness of transmission electron microscopy in cluster characterization is illustrated in Figure 3.²⁰ A thin (~ 50 Å) amorphous carbon film supports an isolated crystallite of PbS. The image of the amorphous film is a speckled background. Superimposed on this background is a localized region of crossed lines, showing distinct dots with regular spacing along the lines. This is an image of a rocksalt-type PbS crystallite looking down a $\langle 100 \rangle$ axis. The line-to-line distance

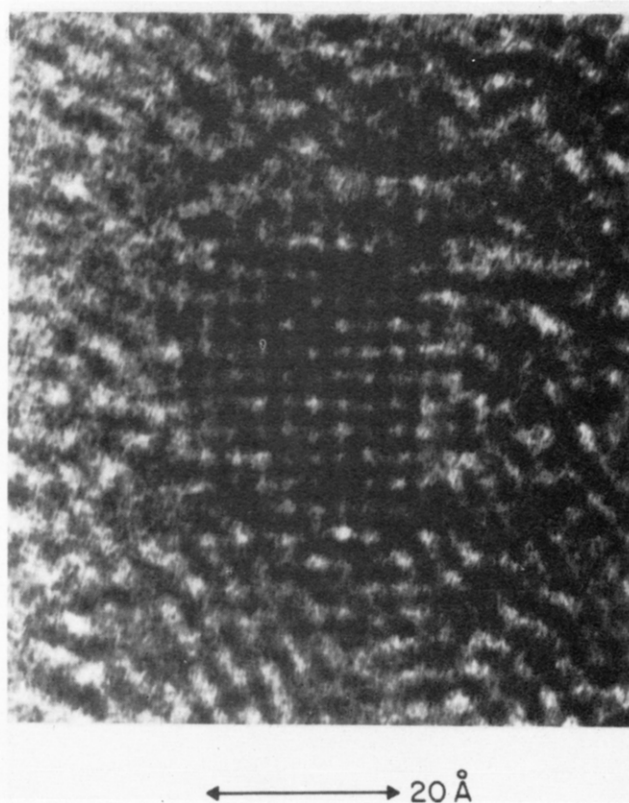


Figure 3. Transmission electron micrograph of a PbS cluster supported on an amorphous carbon film. Adapted from ref 20.

is the PbS bond length, 2.9 ± 0.1 Å. The dots are columns of alternating Pb and S atoms. These images give directly the size and shape distributions. They also demonstrate that the cluster internal structure is crystalline. To my knowledge, in all arrested precipitation clusters where structural characterization has been carried out, the same unit cell and same bond length are found in the cluster as in the bulk material.

There are limits to the knowledge provided by this method. These cross-sectional images show the average internal structure and are not sensitive to possible surface reconstruction. The absolute accuracy in bond length determination is not high either. Nevertheless, the structural knowledge obtained by these techniques enables us to semiquantitatively understand the cluster electronic structure as seen in the next section.

Cluster Molecular Orbitals

The fact that the unit cell is the same in these arrested precipitation clusters as in the bulk materials implies that the cluster MOs evolve into Bloch MOs as size increases. The infinite crystal Bloch MOs have interesting properties that in turn give some insight to the physical nature of cluster MOs. The general form of a Bloch MO is

$$\Phi_{k,\mu}(r) = e^{i\vec{k} \cdot \vec{r}} \chi_{k,\mu}(r) \quad (1)$$

The $\chi_{k,\mu}$ have the periodicity of the unit cell with a relatively weak k dependence. The $e^{i\vec{k} \cdot \vec{r}}$ factor is plane wave-like with a wavelength $\lambda = 2\pi/k$ longer than a unit cell. A Bloch MO of pure \vec{k} is infinitely delocalized, and \vec{k} only becomes a good quantum number in the limit of an infinitely large crystallite. The band structure ($E(k)$ plot for the MOs) of such a semiconductor is shown in Figure 4. An extra electron in this semiconductor sits at the bottom of the conduction band near $k = 0$.

The partial plane wave nature of the Bloch MO suggests approximating a cluster MO $\psi_i(r)$, localized in space, as a Fourier transform wave packet of Bloch MOs:²⁰

$$\psi_i(\vec{r}) = \sum_{\mu} \int_{\mathbf{k}} f_{i\mu}(\mathbf{k}) \Phi_{k,\mu}(\vec{r}) d\mathbf{k} \quad (2)$$

Here μ is an index for summation over different bands. Consider

(30) For example, see Campisano, S. U.; Gibson, J. M.; Poate, J. M. *Appl. Phys. Lett.* **1985**, *46*, 580.

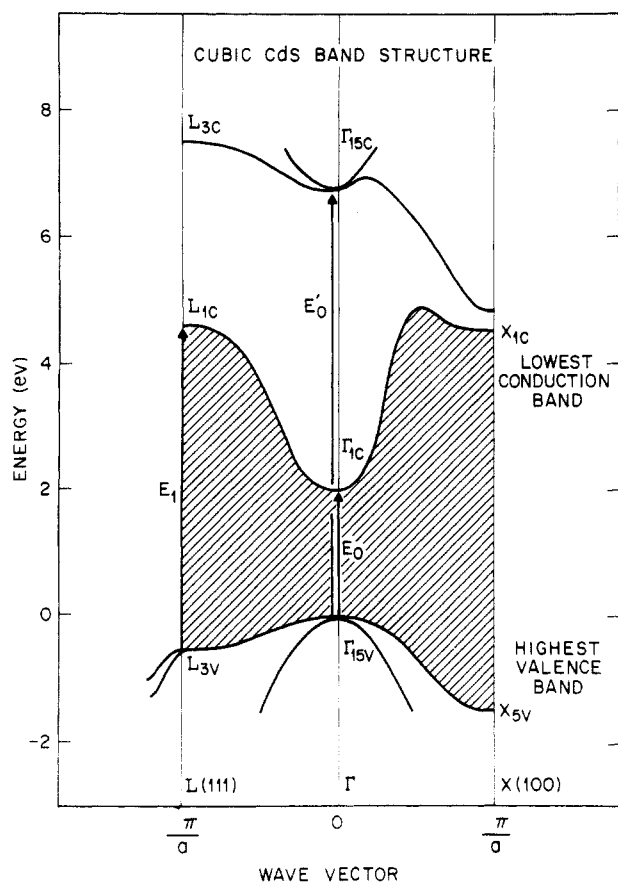


Figure 4. Partial band structure diagram of cubic crystalline CdS. The lines labeled L(111) and X(100) refer to different directions within the unit cell.

a simple example: the LUMO that evolves into the $k = 0$ state at the bottom of the conduction band. As long as the cluster is not too small, only k states from the conduction band itself will contribute to this ψ_i . If we ignore the weak k dependence of χ , then the function $f_i(k)$ should be a simple Gaussian-like distribution of k values in the immediate neighborhood of the asymptotically good quantum number $k = 0$.

The smaller the cluster, the larger the region of k space necessary to localize the electron inside the cluster. The (size-dependent) expectation value of the electron energy is

$$E_i = |\langle \psi_i | \hat{H} | \psi_i \rangle| \simeq E_c + \frac{\pi^2}{2R^2} \sum_{i=x,y,z} \left[\frac{\partial^2 E}{\partial k_i^2} \right] \quad (3)$$

We have kept only the lowest order nonzero term in a Taylor's series expansion for the energy and assumed a spherical cluster. It turns out to be generally true, for expansion about positions of arbitrary k , that first and crossed second derivatives are not important, if the cluster has a compact shape with a center of symmetry.²⁰

This expression has an interesting interpretation. The second derivatives define an effective mass tensor:

$$\bar{M}_{ij} \equiv \hbar^2 / \frac{\partial^2 E}{\partial k_i \partial k_j} \quad (4)$$

at every point on the conduction band. Individual elements may be of arbitrary sign and magnitude. However, near $k = 0$ for the conduction band of most semiconductors, the tensor is nearly isotropic with average diagonal element m_e . We then have

$$E_i \simeq E_c + \frac{\pi^2 \hbar^2}{2m_e R^2} \quad (5)$$

The second term on the right-hand side is essentially the particle-in-a-box quantum energy. This formula has a simple physical

interpretation: the energy of an extra electron in a tiny crystallite is the conduction band energy E_c plus the quantum localization energy of a "pseudoelectron" of effective mass m_e . m_e has no direct relationship to the real electron mass m_0 and is often smaller. For example, in CdS $m_e = 0.18m_0$, in GaAs $m_e = 0.05m_0$, and the in-plane effective mass for a graphite sheet is $\sim 0.004\text{--}0.06m_0$. An electron in a bulk crystal or tiny crystallite moves with an effective mass m_e because, in both cases, the dominant effect is wave diffraction from the atomic lattice. The electron strongly coupled to the lattice is a "pseudoparticle" with effective mass m_e . These simple ideas are valid as long as the unit cell is the same in both cluster and bulk material. Extremely large quantum size effects are possible because the "particle" has a mass that may be far lighter than that of a real electron.³¹

So far we have considered the size-dependent energy of the LUMO, that is, a single electron near the bottom of the conduction band. In a similar fashion, the energy of a missing electron, a "hole", in the HOMO can be approximated. The HOMO energy is a complex problem because there is a significant spin-orbit interaction present in a threefold electronically degenerate valence band in II-VI and III-V zinc blende semiconductors. Nevertheless, under some circumstances the localization energy can be approximated in the same way with a (different) hole effective mass m_h .

It is possible to include electron-hole correlation in a certain special sense, if we further assume, following the standard solid-state ansatz, that the electron and hole interact with each other via a shielded Coulomb interaction. Then the model Hamiltonian for the cluster's lowest excited state is³²

$$\hat{H} = \frac{\hbar^2}{2m_e} \nabla_e^2 + \frac{\hbar^2}{2m_h} \nabla_h^2 - \frac{e^2}{\epsilon|r_e - r_h|} + \text{polarization terms} \quad (6)$$

The polarization terms enter because we must consider the correct form of the Coulomb interaction in the presence of the crystallite surface. An analytical approximation for the lowest eigenvalue (i.e., the first excited electronic state) is

$$E^* \simeq E_g + \frac{\hbar^2 \pi^2}{2R^2} \left[\frac{1}{m_e} + \frac{1}{m_h} \right] - \frac{1.8e^2}{\epsilon R} + \text{smaller terms} \quad (7)$$

This simple formula is possible because the correlation between electron and hole positions, induced by the Coulomb interaction, is not strong. The major effect is additive, independent confinement energies for electron and hole.

The Coulomb term shifts E^* to lower energy as R^{-1} , while the quantum localization terms shift E^* to higher energy as R^{-2} . Thus the apparent band gap will always increase for small enough R —an effect that has now been experimentally observed for many different materials. Another result of eq 7 is an accidental cancellation of the second and third terms for specific values of R . In large band gap materials where the Coulomb term is important, this value is $\approx 85 \text{ \AA}$. In small band gap materials, the Coulomb term is far smaller and the cancellation should not be important.

We show in Figure 5 the predicted asymptotic approach of E^* to E_g for various semiconductors.³² There are no adjustable parameters in the calculations. The interesting aspect is the presence of quantum size effects extending to quite large physical sizes. As mentioned in the Introduction, the source of this slow approach to bulk properties, in the region of the fundamental gap, is strong chemical bonding.

In these materials the valence and conduction bands are typically several electronvolts wide. The valence band to conduction band optical absorption, made up of contributions from all possible values of k , extends from the band gap usually into the vacuum ultraviolet. The effective mass tensor is a very strong function

(31) There is a partial analogy here with the theoretical treatment advanced by Cohen and co-workers for sodium clusters (ref 6). They consider free electrons inside a spherically symmetric well and predict enhanced stabilities when angular momentum electronic shells are completely filled. They use the actual electron mass, as is appropriate for simple free electron type metals.

(32) Brus, L. E. *J. Chem. Phys.* **1984**, *80*, 4403.

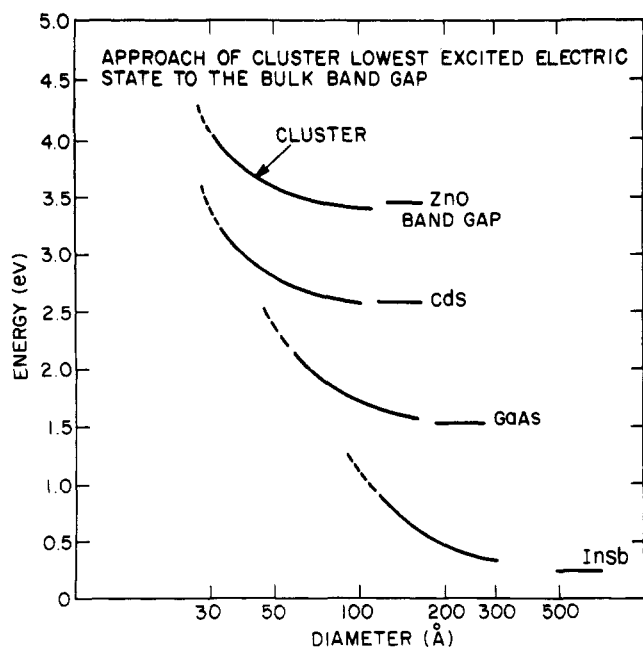


Figure 5. Calculated energy of the cluster lowest excited electronic state in relation to the bulk band gap. Adapted from ref 31.

of k (i.e., position within the Brillouin zone) for both valence and conduction bands. One can use the Fourier transform argument to predict how localization will shift energies at arbitrary positions within the Brillouin zone.²⁰ This argument predicts that it is not the absolute value of k that controls localization, but the local effective mass. It should systematically be true that both valence and conduction bands will contract toward their centers of gravity as localization proceeds. As a general consequence, optical absorption far above the gap should be relatively size insensitive, as opposed to the gap itself. This general relationship has now been observed in clusters of many materials made by the "arrested precipitation" technique.

A related question is the dependence of ionization potential on size. This can be modeled by combining the size dependence of the HOMO (as previously described) with the size-dependent electrostatic energy of a charged dielectric sphere.^{13,33} The results are interesting. In this case the R^{-1} electrostatic term and the R^{-2} quantum size term have the same sign, both decreasing the ionization potential in small crystallites. There do not appear to be any experimental measurements of vacuum ionization potentials for small crystallites. In colloids the equivalent parameters are the redox potentials of holes and electrons. Experimental reports have just begun to appear indicating that these redox potentials are size dependent.³⁴ This phenomenon opens the possibility of controlling liquid-phase photochemical processes via crystallite size. A problem that must be overcome is enhanced photodissociation of the crystallite itself, if these clusters are to be used as stable photosensitizers. Photodissolution becomes more pronounced in smaller clusters as excited-state energies increase, and the binding energies per atom decrease.

Further "Localization"

So far we have used "localization" to imply electron confinement with a cluster, in a state that has population density throughout the cluster. If the cluster has point defects and/or surface states, then further localization is possible. Figure 6 is a schematic correlation diagram of the different states that should exist in both bulk semiconductors and small clusters.³⁵ In bulk materials defect states are broadly divided into deep and shallow traps. Deep traps are essentially localized in space at a lattice site defect and

SPATIAL ELECTRONIC STATE CORRELATION DIAGRAM

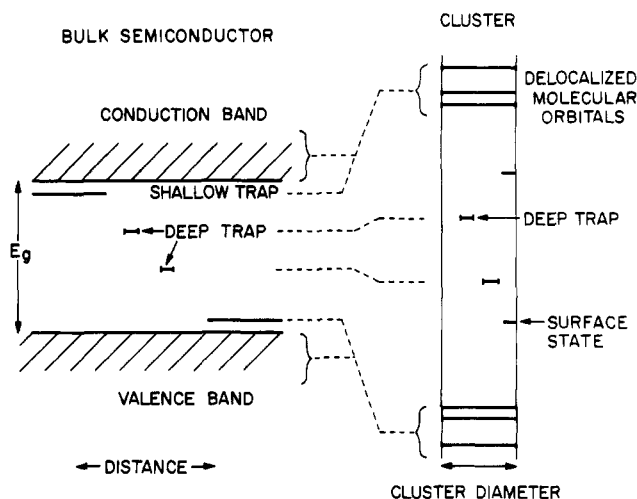


Figure 6. Schematic correlation diagram relating cluster states to bulk crystal states.

lie in the middle of the band gap. Shallow traps lie within a few millielectronvolts of the corresponding band edge and can be described by a hydrogenic model where the mobile charge orbits the trap in a large $1S$ orbit of radius α

$$\alpha = \frac{\epsilon}{m^*/m_0} a_0 \quad (8)$$

Here a_0 is the hydrogen Bohr radius, 0.53 Å. If ϵ is large and m^* small, then α can be quite large. In the figure, shallow traps are represented by a long line, implying delocalization over several unit cells.

As crystallite size decreases, shallow traps will respond to small size before deep traps and shift to higher energy. When crystallite size becomes commensurate with α , the distinction between shallow traps and the Fourier transform states ceases. The trap Coulomb potential is felt by all states delocalized over the cluster. The net result is that the energy range between deep traps and the cluster delocalized states should open up in small crystallites as shown in the figure.³⁵

The interpretation of the optical absorption spectra advanced so far does not involve trap states. The lowest HOMO \rightarrow LUMO transition is expected to have an oscillator strength near one,³² and the size dependence of the observed spectra strongly supports the idea that cluster Fourier transform states given by eq 2 and 7 dominate the spectra. Sometimes a "tail" is observed below the exciton absorption; this may represent absorption by trapped carriers. However, the luminescence of CdS clusters clearly involves trapped carriers and is described in the next section.

Cluster Luminescence

A major difference exists between metal clusters and semiconductor clusters. Transition-metal clusters with 10 or more atoms already have an extremely high density of electronic states above the HOMO. The limited evidence available to date indicates that creation of excited states is followed by ultrafast electronic to vibrational radiationless transition. To my knowledge there are no reports of long-lived excited states or luminescence.

Semiconductor clusters typically have $S_1 \rightarrow S_0$ energy gaps of several electronvolts, as we have seen, neglecting the presence of trap and surface states. Direct $S_1 \rightarrow S_0$ internal conversion is a very high order process in lattice phonons ($\hbar\omega_{\text{vib}} \sim 100\text{--}300\text{ cm}^{-1}$) and should be slow. In fact CdS cluster luminescence is detectable at room temperature^{17,18,36} and quite strong at cryogenic temperatures.³⁴ Excited-state lifetimes in excess of $2 \times 10^{-4}\text{ s}$ occur at $T \leq 20\text{ K}$. This emission is not $S_1 \rightarrow S_0$ luminescence, however,

(33) Brus, L. E. *J. Chem. Phys.* **1983**, *79*, 5566.

(34) Nedeljkovic, J. M.; Nenadovic, M. T.; Mićić, O. I.; Nozik, A. J. *J. Phys. Chem.* **1986**, *90*, 12.

(35) Chestnoy, N.; Harris, T. D.; Hull, R.; Brus, L. E. *J. Phys. Chem.*, in press.

(36) Papavassiliou, G. C. *J. Solid State Chem.* **1981**, *40*, 330.

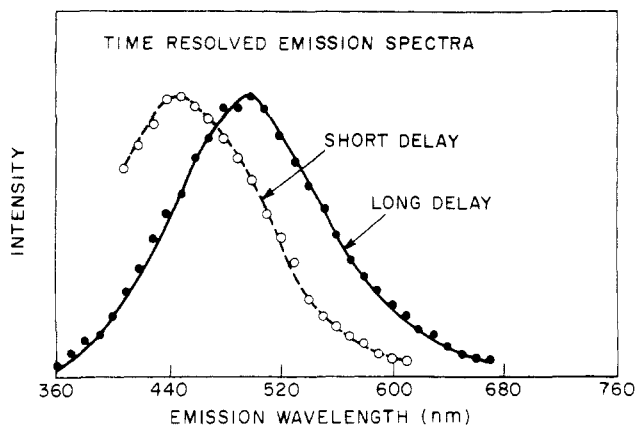


Figure 7. Time-resolved emission spectra of luminescence from ≈ 22 -Å CdS clusters in a frozen organic glass at ≈ 10 K, adapted from ref 34. Short delay refers to the period $0-1.5 \times 10^{-6}$ s, and long delay to the period $(17-34) \times 10^{-6}$ s. There is no resolvable vibronic structure at ~ 1 -Å resolution under the present conditions.

which should have a purely radiative lifetime of $\approx 10^{-9}$ s. The broad emission spectrum in Figure 7 and the temperature dependence of the lifetimes indicates that the electrons are strongly coupled to lattice phonons.³⁵ The long lifetimes indicate that the hole and electron are separately trapped at different locations in the crystallite. Decay at low temperature occurs by a combination of radiative and nonradiative tunneling of the electron back to the hole.

In the luminescence spectra, there is a correlation between the emission wavelength and the rate of decay. Faster emission occurs

at higher energy. In this correlation the basic variable seems to be primarily the distance between traps and not cluster size.³⁵ Closely trapped pairs emit at higher energy because of the ground-state Coulomb attraction which exists between traps of opposite charge. They also tunnel faster due to a greater exchange (wave function overlap) matrix element. The excited-state decay properties seem to be determined by *pairs* of trapped carriers and not by isolated trap (i.e., defect) electronic states. In this sense they bear some resemblance to molecular states, specifically to the biradical states often observed in organic chemistry.³⁷

Final Remarks

Metal and semiconductor clusters represent entire new classes of large molecules. Their structural and dynamical properties contain novel aspects and should be of interest to the molecular spectroscopy and chemical physics communities. Our understanding of their chemistry and physics is growing rapidly, yet remains primitive. I believe that the potential for additional interesting discoveries is present. It is already clear that semiconductor clusters must grow to a very large physical size before bulk electronic and optical properties are present. The clusters themselves may find useful chemical and optical applications.

Acknowledgment. It is a great pleasure to acknowledge the essential contributors of my collaborators—J. M. Gibson, R. Hull, and S. Nakahara in electron microscopy; and R. Rossetti, N. Chestnoy, and T. D. Harris in synthesis and luminescence spectroscopy. K. Ragavachari, T. D. Harris, and C. J. Sandroff offered valuable suggestions on an earlier version of this manuscript.

(37) Turro, N. J. *Modern Molecular Photochemistry*; Benjamin/Cummings: Menlo Park, CA, 1978; Section 7.8.

SPECTROSCOPY AND STRUCTURE

α -Helical Polypeptide Circular Dichroism Component Band Analysis

David A. Rabenold[†] and William Rhodes^{*‡}

Institute of Molecular Biophysics and Department of Chemistry, The Florida State University, Tallahassee, Florida 32306 (Received: June 24, 1985; In Final Form: January 27, 1986)

Equations are presented for calculating circular dichroism component bands for short helical polymers. Also presented are equations for calculating the effect of high-frequency transitions, which are approximated by transition moment dyadics, on the low-frequency region of the spectra. For a rigid model of an α -helix calculations show the following: (1) The isotropic part of the transition moment dyadic for high-energy transitions located on the amide is responsible for large induced long-wavelength circular dichroism contributions. (2) The net long-wavelength circular dichroism helix band is skewed with the negative high-frequency lobe being significantly reduced in intensity in comparison to the unperturbed helix band. (3) The chain length dependence of the circular dichroism is largely due to that of the helix band.

I. Introduction

Calculations of the circular dichroism (CD) of helical polypeptides have been successful to various degrees, e.g., for the α -helix¹⁻⁵ and for poly-L-proline (II).⁵⁻⁷ Theoretical formulations of the CD for infinitely long helices with two transitions per chromophore, the $\pi\pi^*$ and the $n\pi^*$, predict a conservative spectrum with five or six bands, namely one helix band, two radical

bands, and the $n\pi^*$ band which is balanced in intensity by a contribution(s) at the position of one or both radial bands.^{8a}

- (1) (a) R. W. Woody, *J. Chem. Phys.*, **49**, 4797 (1968); (b) R. W. Woody and I. Tinoco, Jr., *J. Chem. Phys.*, **46**, 4927 (1967).
- (2) F. M. Loxsom, L. Tterlikkis, and W. Rhodes, *Biopolymers*, **10**, 2405 (1971).
- (3) J. Applequist, *J. Chem. Phys.*, **71**, 4332 (1979).
- (4) E. S. Pysh, *J. Chem. Phys.*, **52**, 4723 (1970).
- (5) E. W. Ronish and S. Krimm, *Biopolymers*, **13**, 1635 (1974).
- (6) J. Applequist, *Biopolymers*, **20**, 2311 (1981).

[†] Institute of Molecular Biophysics.

[‡] Institute of Molecular Biophysics and Department of Chemistry.